ResearchGate

See discussions, stats, and author profiles for this publication at: https://www.researchgate.net/publication/215559950

Adsorption and Dissociation of Phosphine on Si(001)

ARTICLE *in* THE JOURNAL OF PHYSICAL CHEMISTRY · MARCH 1996

Impact Factor: 2.78 · DOI: 10.1021/jp952452h

CITATIONS
70

READS
58

3 AUTHORS, INCLUDING:

Robert J. Hamers
University of Wisconsin–Madison
386 PUBLICATIONS **17,300** CITATIONS

SEE PROFILE

Available from: Robert J. Hamers
Retrieved on: 26 January 2016

Adsorption and Dissociation of Phosphine on Si(001)

Jun Shan, Yajun Wang, and Robert J. Hamers*

Department of Chemistry, University of Wisconsin, 1101 University Avenue, Madison, Wisconsin 53706

Received: August 18, 1995; In Final Form: December 21, 1995[⊗]

The adsorption and thermal decomposition of phosphine (PH_3) on the Si(001) surface has been investigated using Fourier transform infrared spectroscopy. Phosphine is found to adsorb both nondissociatively and dissociatively, depending on the coverage and flux during exposure. Infrared spectra reveal that PH_3 dissociates to produce two distinct forms of PH_2. Further decomposition yields phosphorus atoms and surface hydrogen. The surface P atoms form P−Si heterodimers and, in the presence of surface hydrogen, form PSiH "hydrided heterodimers". The bonding of hydrogen in this form is stronger than on the clean Si surface, resulting in a higher desorption temperature for hydrogen when phosphorus is present on the surface. Molecular orbital calculations are used to provide insight into the bonding geometry of PH_3 on Si(001).

1. Introduction

In chemical vapor deposition (CVD) processes, dopants are typically introduced through thermal decomposition of hydride-based precursors. In addition to their primary role in controlling the electrical characteristics of semiconductor thin films, the presence of dopants on the surface changes the surface free energy as well as the surface chemical reactivity, strongly influencing both the growth rate and surface morphology in CVD processing. In phosphorus doping of silicon, the thermal decomposition of phosphine (PH_3) in the CVD gas stream strongly decreases the growth rate; yet, incorporation of phosphorus into the bulk is relatively inefficient.[1−4]

Several previous studies have investigated the interaction of PH_3 with Si(111) and Si(001) surfaces. On the Si(111) surface,[5−10] electron energy loss spectroscopy studies have shown that PH_3 dissociates on Si(111) at temperatures as low as 120 K, producing a distinct PH_2 wagging mode vibration.[8,9] Yu, Meyerson, and co-workers[11−14] first studied the interaction of PH_3 with Si(001) using secondary ion mass spectroscopy (SIMS), Auger electron spectroscopy (AES), X-ray photoelectron spectroscopy (XPS), temperature-programmed desorption (TPD), and low-energy electron diffraction (LEED). On the basis of their observations of two distinct core−level shifts for phosphorus and a sharp (2×1) LEED pattern persisting after PH_3 exposure, they concluded that on Si(001) most PH_3 molecules adsorbed without dissociation. They proposed a bonding configuration in which the PH_3 molecule was centered above the Si═Si surface dimers, allowing the PH_3 lone pair electrons to interact with the π electron system of the Si═Si dimers.

In scanning tunneling microscopy (STM) studies,[15,16] we found that STM images of Si(001) exposed to PH_3 indeed showed protrusions locally ordered into small c(4×2) domains, which we attributed to PH_3 molecularly adsorbed on the Si dimers in the configuration proposed by Yu et al. However, we also found that the ordering was comparataively poor and that vacancy defects on the surface were considerably enlarged after PH_3 exposure, suggesting that defects might play an important role in the chemistry of PH_3 on Si(001). At higher temperatures, we found that PH_3 dissociated and that the phosphorus atoms were dispersed on the surface, at moderate P coverages preferring to form P−Si heterodimers and only at high coverage forming P−P dimers.

Recently, controversy has arisen regarding the interaction of PH_3 with Si(001). While our STM studies suggested molecular adsorption of PH_3 in an "on-top" configuration, Cao et al.[17] performed molecular orbital calculations of the PH_3/Si(001) system and found that the "on-top" bonding configuration for molecular PH_3 was less favorable than having PH_3 molecularly adsorbed on one end of a Si−Si dimer in the "dangling bond" position. Additionally, Colaianni and co-workers recently investigated the PH_3/Si(001) system using high-resolution electron energy loss spectroscopy (HREELS) and TPD.[18] After exposure of Si(001) to PH_3 at 300 K, they observed both Si−H vibrations and a characteristic PH_2 wagging mode in high-resolution electron energy loss spectroscopy (HREELS), showing that some PH_3 dissociates upon interaction with Si(001).

In order to better understand the chemistry of this technologically important dopant on Si(001), we have investigated its adsorption and thermal dissociation of PH_3 on Si(001) using Fourier transform infrared spectroscopy in conjunction with ab initio molecular orbital calculations. Our infrared results show that at 300 K both nondissociative (molecular) and dissociative adsorption of PH_3 occur on Si(001). Moreover, we show that the relative amounts of molecular vs dissociative adsorption is dependent on the exposure flux and that a substantial fraction of the molecules can be molecularly adsorbed under suitable exposure conditions. Ab initio results show that the molecular adsorption of PH_3 is enhanced by dimer tilting, which produces nucleophilic and electrophilic reaction sites. Finally, we investigate the thermal decomposition of PH_3 on clean and phosphorus-enriched Si(001) to gain further insight into the mechanism of thermal decomposition. Our results provide new evidence for a number of well-defined phosphorus-containing species on the Si(001) surface.

2. Experimental Section

The experiments were conducted in an ultrahigh-vacuum (UHV) chamber (base pressure 1×10^{-10} Torr) equipped with a mass spectrometer for residual gas analysis and a precision leak valve for admitting gases in controlled quantities. For the infrared studies, we use a multiple internal reflection geometry. Light from a Fourier transform infrared spectrometer (Mattson, RS-1000) passes through a rotatable wire-grid polarizer, is focused using a 5 in. focal length parabolic mirror, and enters the chamber through a BaF_2 window. This light enters the narrow, polished edge of a $20 \times 9 \times 0.6$ mm^3 Si(001) sample at an angle of approximately 56° with respect to the large (001)

* To whom correspondence should be addressed.

[⊗] Abstract published in *Advance ACS Abstracts,* March 1, 1996.

0022-3654/96/20100-4961$12.00/0 © 1996 American Chemical Society

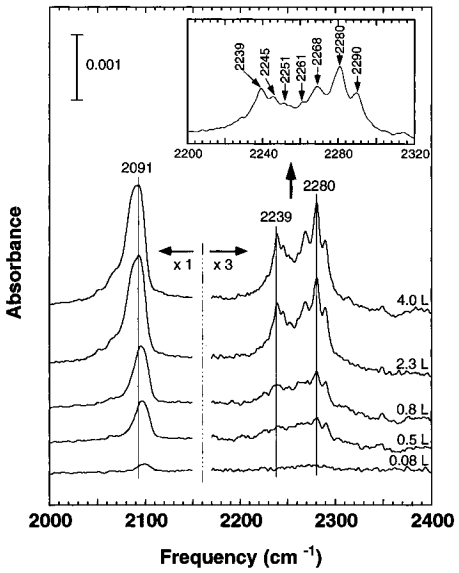

Figure 1. p-polarized infrared absorption spectra of phosphine on Si-(001) at various exposures. Exposure pressure = 5×10^{-9} Torr.

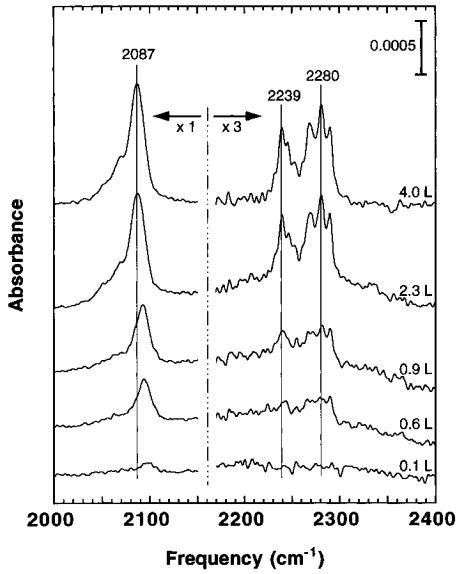

Figure 2. s-polarized infrared absorption spectra of phosphine on Si-(001) at various exposures. Exposure pressure = 5×10^{-9} Torr.

plane and undergoes multiple internal reflection down the 2 cm length, resulting in approximately 30 reflections from the sample surfaces. The light emerging from the other end is collected and focused onto the InSb detector element (IR Associates) using an off-axis parabolic mirror. The spectrometer and all of the optics were purged with purified nitrogen. Spectra were collected at 300 K, typically using 2 cm^{-1} resolution and signal averaging between 1600 and 4000 interferograms. For each experiment, a spectrum of the clean Si(001) surface was taken and used as a reference for subsequent spectra.

Samples were cut from double-polished Si(001) wafers (B-doped, 11−25 Ω cm). The 9×0.6 mm^2 edges were polished at a 45° angle with respect to (001) to achieve an optically smooth surface, and the samples were then cleaned in acetone and methanol before being clamped onto the sample holder using two tantalum wires. Samples were exposed to an ozone-producing ultraviolet lamp for 5 min to reduce surface carbon contamination and then transferred to the UHV chamber through a load lock. The samples were degassed at 810 K for 12 h and then annealed at 1400 K for several seconds on a separate heating stage while maintaining the chamber pressure $<10^{-9}$ Torr. After cooling for approximately 20 min, samples were transferred to a position for infrared spectroscopy measurements. The samples could be heated to moderate temperatures in this position, permitting thermal decomposition studies to be performed without moving the sample and thereby ensuring a constant "reference" background for all spectra. Temperatures above 900 K were measured using an infrared pyrometer. Temperatures below 900 K were measured by recording the sample power dissipation during heating and calibrating the temperature as a function of applied power in vacuo at the conclusion of the experiment using a small chromel−alumel thermocouple. This procedure produces temperatures believed accurate to within 50 K while maintaining the cleanest possible samples during the experiments. In order to ensure that PH_3 was not dissociated by hot filaments in the vacuum chamber, there was no line of light from the sample to any filament, and the use of heated filaments was kept to an absolute minimum.

3. Results

Adsorption of PH_3 on Si(100) at Room Temperature. Figure 1 shows infrared absorption spectra as a function of coverage for Si(001) exposed to PH_3 at a pressure of 5×10^{-9} Torr. Figure 1 was obtained using p-polarized light; due to the 56° angle of incidence, this is capable of exciting transition dipoles both parallel and perpendicular to the surface plane. In Figure 1, two major spectral regions can be discerned. The range from 2040 to 2110 cm^{-1} arises from Si−H stretching vibrations, while the range from 2230 to 2300 cm^{-1} arises from P−H stretches. The detection of Si−H stretching vibrations immediately after exposing Si(001) to PH_3 demonstrates that the interaction of PH_3 with Si(001) is at least partially dissociative, in agreement with recent results by Colaianni et al.[18] using HREELS. With the higher resolution available with infrared spectroscopy, however, it is possible to delineate a number of different chemical forms of phosphorus and silicon on the surface based on the vibrational frequencies of the Si−H and P−H stretching modes.

Within the PH spectral range 2230−2300 cm^{-1}, the absorption features naturally divide into two groupings. Group I consists of a set of three peaks at 2290, 2280, and 2268 cm^{-1}, while group II consists of a set of four peaks at 2239, 2245, 2251, and 2261 cm^{-1}. Another small peak can sometimes be detected near 2254 cm^{-1}, but its intensity is usually too small for analysis. As the exposure is increased, Figure 1 shows that all peaks increase monotonically in height, reaching a maximum value after exposure to approximately 3 langmuirs of PH_3; further exposure induces no further changes in the wavelength or absorption strengths of the peaks. Within the Si−H stretching region, Figure 1 shows that at low exposure a single broad peak is observed near 2100 cm^{-1}. As the coverage is increased, this peak increases in intensity and shifts slightly; at saturation exposure it is barely resolvable into two peaks with maxima near 2087 and 2099 cm^{-1}.

Insight into the origins of these peaks can be obtained by comparing s-polarized and p-polarized absorption spectra. Figure 2 shows s-polarized spectra as a function of exposure. Within the P−H spectral region, the same peaks are observed with s-polarized light (Figure 2) as with p-polarized light (Figure 1). However, some changes are observed in the relative intensities. In particular, within the group I P−H peaks, for p-polarized light the central peak at 2280 cm^{-1} is nearly twice as high as the peaks at 2290 and 2268 cm^{-1}, while for

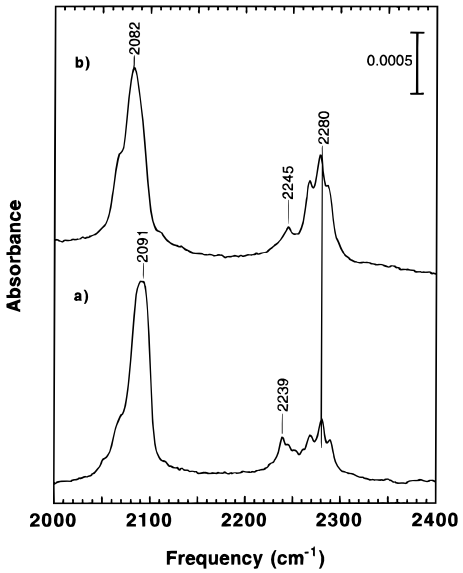

Figure 3. Dependence of PH_3/Si(001) infrared absorption spectra on flux used to achieve saturation exposure: (a) exposure pressure $= 5 \times 10^{-9}$ Torr; (b) exposure pressure $= 1 \times 10^{-6}$ Torr.

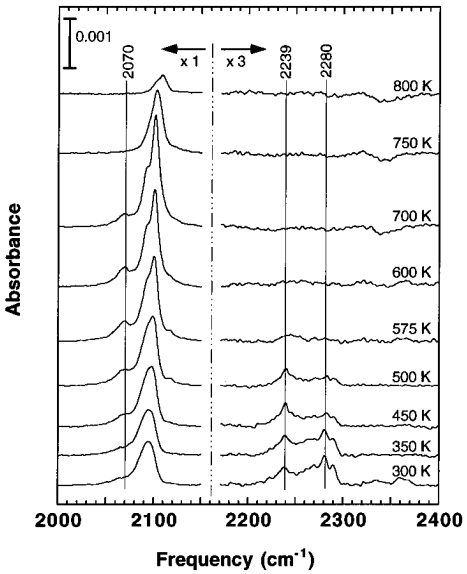

Figure 4. Influence of annealing on p-polarzed infrared absorption spectrum of medium-coverage (1.2 langmuirs total exposure at $P = 5 \times 10^{-9}$ Torr) PH_3 on Si(001). All spectra were taken at 300 K after annealing to the indicated temperature for 1 min.

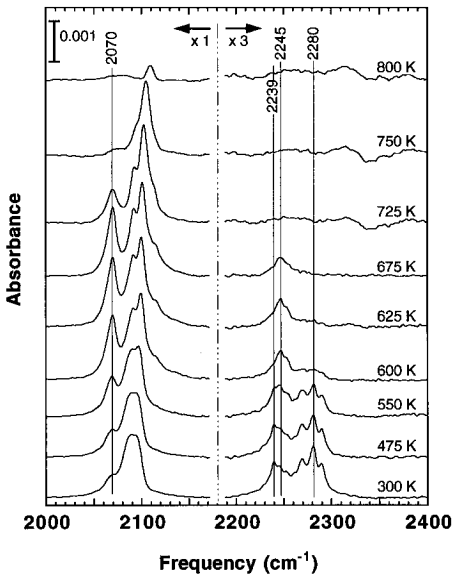

Figure 5. Influence of annealing on p-polarized infrared absorption spectrum of saturation-coverage (10 langmuirs total exposure at $P = 5 \times 10^{-9}$ Torr) PH_3 on Si(001). All spectra were taken at 300 K after annealing to the indicated temperature for 1 min. p-polarized spectra are shown.

s-polarized light all three peaks show comparable absorption strengths. Polarization-dependent changes are also visible for the Si−H features: whereas the p-polarized spectrum shows a broad doublet at 2087 and 2099 cm^{-1}, the s-polarized spectrum shows a single large peak at 2087 cm^{-1}.

The chemical composition of the PH_3-saturated surface is also strongly dependent on the *rate* of exposure. Figure 3a, shows a p-polarized FTIR spectrum of a Si(001) surface saturated slowly at a pressure of 5×10^{-9} Torr (Figure 3a), while Figure 3b shows an equivalent spectrum for a surface saturated quickly at a pressure of 1×10^{-6} Torr (Figure 3b). Within the PH spectral region, a high flux (rapid exposure) substantially increases the absorbance from the three group I peaks at 2268, 2280, and 2290 cm^{-1} by more than 50%, while simultaneously decreasing slightly the area of the group II and Si−H spectral regions. Minor differences are also observed in the relative intensities within the group II peaks and in the Si−H region. While at low flux the predominant group II peak is at 2239 cm^{-1}, at higher flux the predominant group II peak is at 2245 cm^{-1}. This 2245 cm^{-1} peak persists the strongest group II peak as the sample is annealed to higher temperatures (not shown). Within the Si−H spectral region, low flux produces two barely resolved peaks centered at 2091 cm^{-1}, while high flux produces a single broader peak near 2082 cm^{-1} and a low-frequency shoulder. This dependence on incident flux suggests that dissociation of the molecule or molecular fragment responsible for the group I peaks occurs on the time scale of the exposure (several minutes), so that higher flux rates are able to stabilize certain metastable species.

Thermal Decomposition on PH_3 on Si(001). Further insight into the adsorption and dissociation process comes from experiments in which PH_3-exposed samples are annealed to induce thermal decomposition. Figures 4−6 show specific annealing sequences, while Figures 7 and 8 summarize changes in specific absorption peaks.

Figure 4 shows a sequence obtained after exposure to 1.2 langmuirs PH_3 (moderate coverage) using p-polarized light. This sequence shows that annealing to 350 K leaves the spectrum unaffected, but after annealing between 350 and 450 K there is a substantial decrease in the group I peaks, a substantial increase in the group II peaks (particularly the 2239 cm^{-1} peak), and an increase in the SiH peaks near 2070 and 2099 cm^{-1}. Both the group I and group II peaks decrease in intensity after annealing to 500 K and are absent above 600 K; concurrently, the Si−H peaks at 2070, 2087, and 2099 cm^{-1} increase substantially. Annealing above 725 K leads first to removal of the 2070 cm^{-1} Si−H peak and then sharpening of the remaining Si−H lines into a single line which shifts toward 2110 cm^{-1} as the hydrogen desorbs from the surface.

As noted above, the IR spectra are also dependent on coverage. Figures 5 and 6 shows the effect of annealing a PH_3-saturated surface measuring using p-polarized (Figure 5) and s-polarized (Figure 6) light. Although qualitatively similar to the results at lower coverage, there are some significant differences in both P−H and Si−H regions. At high coverage the group I P−H features are stable to higher temperature (500−550 K in Figure 5) than on surfaces with lower coverage (400 K in Figure 4). Likewise, the group II P−H features are also

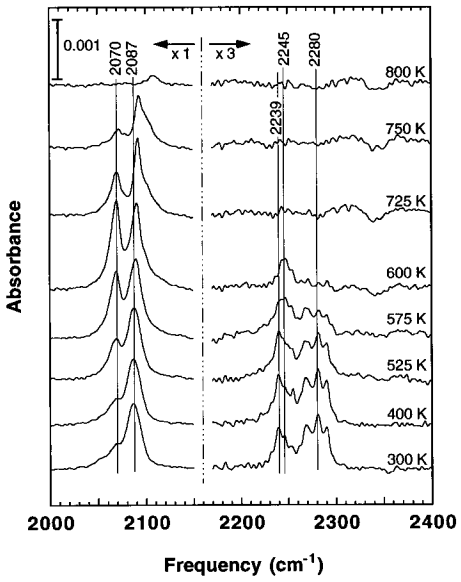

Figure 6. Influence of annealing on s-polarzed infrared absorption spectrum of saturation-coverage (10 langmuirs total exposure at $P = 5 \times 10^{-9}$ Torr) PH_3 on Si(001). All spectra were taken at 300 K after annealing to the indicated temperature for 1 min.

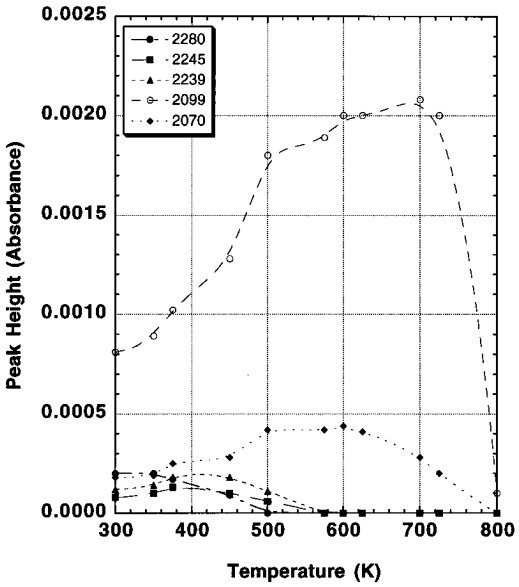

Figure 7. Dependence of individual infrared peak heights on annealing temperature for medium-coverage (1.2 langmuirs total exposure at $P = 5 \times 10^{-9}$ Torr) PH_3 on Si(001).

stabilized at high PH_3 exposure and do not disappear until temperatures of >675 K. A closer comparison of the P−H region between Figure 5 and Figure 4 also shows some differences in relative intensities of the group II P−H features. While at high coverage (Figure 5) annealing to $T > 550$ K increases primarily the P−H peak at 2245 cm^{-1}, at lower coverage (Figure 4) the peak at 2239 cm^{-1} predominates. Within the Si−H region, dissociation of the PH_x species at high coverage at $T > 550$ K leads to a large increase in the 2070 cm^{-1} Si−H peak. This increase is much more pronounced on the high-coverage sample (Figure 5) than at lower coverage (Figure 4). As the annealing temperature is further increased to >675 K, the 2070 cm^{-1} peak decreases, the 2087 and 2099 cm^{-1} peaks sharpen, and at $T > 800$ K only a single Si−H line near 2112 cm^{-1} is observed. Similar changes are observed using s-polarized light (Figure 6); here the increase in the Si−H feature at 2087 cm^{-1} after annealing to $T > 575$ K is particularly apparent.

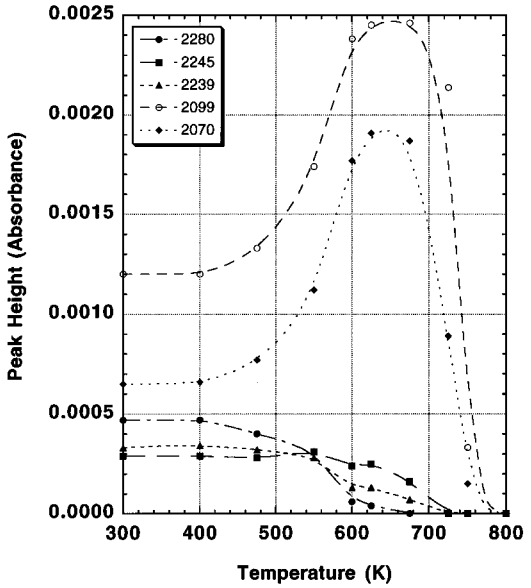

Figure 8. Dependence of individual infrared peak heights on annealing temperature for saturation-coverage (10 langmuirs total exposure at $P = 5 \times 10^{-9}$ Torr) PH_3 on Si(001).

Figures 7 and 8 summarize some of these temperature-dependent changes in the surface chemical composition. Because of the presence of overlapping peaks in many cases, this plot shows only the peak intensities of the best-resolved peaks, with no attempt to deconvolve the spectra.

Influence of Surface Phosphorus on PH_3 Adsorption and Dissociation. In previous studies of the PH_3/Si(001) system using scanning tunneling microscopy,[15,16] we showed that room-temperature exposure of Si(001) to PH_3 results in a maximum phosphorus coverage of 0.2−0.25 monolayer. Upon annealing, however, we showed that phosphorus atoms produced by dissociation of PH_3 do not adsorb on top of the surface, but instead displace Si atoms from the Si═Si dimers of the surface plane, thereby forming large numbers of P−Si "heterodimers". To show how such surface phosphorus enrichment might modify the surface chemistry, we investigated the adsorption and dissociation of PH_3 on Si(001) surfaces which were specifically prepared to contain large numbers of these heterodimers. This was accomplished using successive exposure−anneal cycles; in each cycle the surface was exposed to saturation with PH_3 at 300 K, followed by annealing to 800 K. Each cycle replaces approximately 20% of the remaining surface Si atoms with phosphorus atoms in the form of Si−P "heterodimers" or P−P "homodimers", as described in our previous work.[15] These P-enriched surfaces were then cooled to room temperature and used as the "reference" samples for infrared studies in which PH_3 was allowed to interact with the P-enriched Si(001) surfaces.

Figure 9a shows the IR spectrum produced by the interaction of PH_3 with clean Si(001) at 300 K, while Figure 9b−d shows corresponding spectra obtained on P-enriched surfaces with surface-layer phosphorus coverages estimated at approximately 0.2 (Figure 9b), 0.4 (Figure 9c), and 0.6 (Figure 9d) monolayer. Finally, Figure 9e shows the spectrum obtained after annealing the sample used in (e) to 700 K to induce thermal dissociation. A copmarison of parts a−d of Figure 9 shows that as the surface phosphorus coverage increases, the amounts of all P−H and Si−H species decrease, demonstrating a clear decrease in the overall surface reactivity. In addition, there are significant changes in the shapes of the Si−H and P−H spectral features. At high surface phosphorus concentration (Figure 9d) the group II P−H spectral features are completely absent, and the splitting

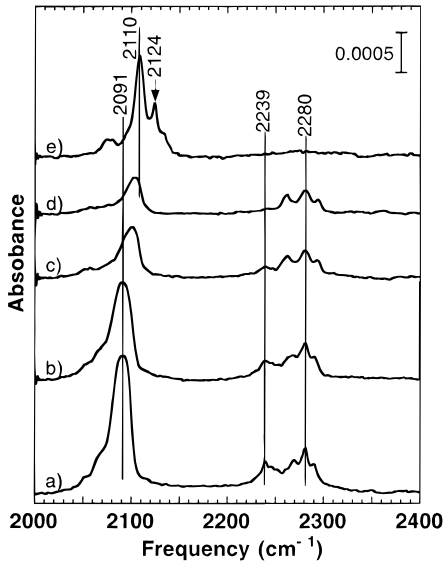

Figure 9. p-polarized infrared absorption spectra for PH_3 interacting with phosphorus-enriched Si(001): (a) 5 langmuirs PH_3 on clean Si-(001); (b) 5 langmuirs PH_3 on Si(001) enriched with 0.2 monolayer of phosphorus; (c) 5 langmuirs PH_3 on Si(001) enriched with 0.4 monolayer of phosphorus; (d) 5 langmuirs PH_3 on Si(001) enriched with 0.6 monolayer of phosphorus; (e) thermal decomposition of surface from (d), induced by annealing (d) to 700 K for 1 min.

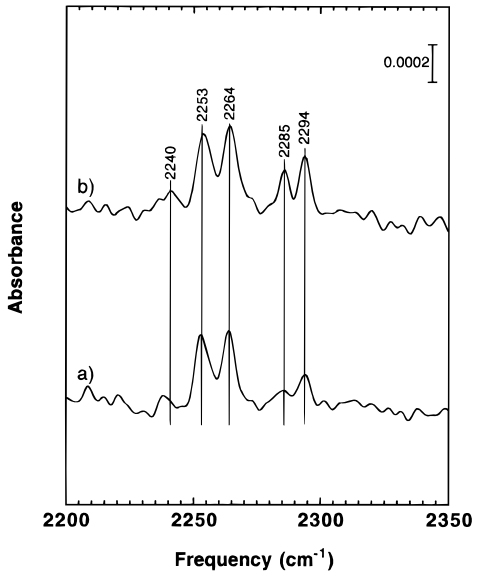

Figure 10. FTIR spectra of Si(111)-(7×7) surface exposed to PH_3: (a) 9 langmuirs exposure and (b) 56 langmuirs exposure (saturation coverage).

between the three peaks constituting the group I P−H features is increased compared with the clean surface. In the Si−H region, the broadened peak near 2091 cm^{-1} is replaced by a peak at 2104 cm^{-1}, similar in frequency to the Si−H peak observed after annealing PH_3-exposed Si(001) surfaces. Finally, Figure 9e shows that, upon annealing of PH_3 adsorbed on the highly P-enriched Si(001) surface, a new, sharp Si−H stretch is observed at 2124 cm^{-1}.

Comparison of FTIR Spectra for PH_3 on Si(001) and Si-(111). In order to help identify the species present on the surface, we also conducted some experiments on Si(111)-(7×7). Figure 10 shows FTIR spectra obtained after exposing a Si-(111)-(7×7) surface to PH_3. At saturation coverage (Figure 10b), four large peaks can be observed at 2253, 2264, 2285, and 2294 cm^{-1}, with evidence for a fifth small peak at 2240 cm^{-1}. At lower coverage (Figure 10a), these same five peaks are observed, but the 2253 and 2264 cm^{-1} peaks appear to predominate at low coverage. The Si−H region (not shown) shows some broad features which might be attributed to Si−H; however, the adsorption of PH_3 on Si(111) changes the surface dielectric constant, making it difficult to distinguish between changes in background and true, broad Si−H absorption features. Previous studies by Wallace et al.[9] and by Taylor et al.[8] have concluded that the interaction of PH_3 with Si(111)-(7×7) produces a mixture of molecular PH_3 and dissociated PH_2 fragments, with the amount of molecular PH_3 increasing as the total surface coverage increases. This in turn suggests that the peaks at 2285 and 2294 cm^{-1} most likely arise from molecularly adsorbed PH_3, and the peaks at 2253 and 2264 cm^{-1} arise from adsorbed PH_2. Molecularly adsorbed PH_3 might give rise to either two or three vibrational frequencies, depending on whether the C_{3v} symmetry is retained or broken. While on Si(111) the molecule can retain its 3-fold symmetry, on Si(001) this is not possible, and three peaks are expected.

Quantum Chemistry Calculations for the PH_3 + Si(001) System. To investigate the energetics of PH_3 interacting with the Si(001) surface, we performed ab initio molecular orbital calculations[19] for molecularly adsorbed PH_3. The silicon surface was modeled starting from a $Si_{21}H_{20}$ cluster containing three surface dimers, the eight underlying atoms in the second layer, four atoms in the third layer, and three Si atoms in the fourth layer. The cluster geometry was first optimized using a $Si_{24}H_{32}$ cluster formed by adding a SiH_2 group atop each dimer in the first layer of the Si_{21} cluster, terminating all "dangling bonds" with H atoms, and then performing a complete geometry optimization in which bond lengths and angles between all atoms are allowed to completely adjust to minimize the total system energy. In subsequent calculations, the topmost SiH_2 groups and H atoms terminating the dimers were removed and various adsorbate groups and/or substitutions were made; the hydrogen atoms were then kept *fixed* at their optimized values from the $Si_{24}H_{32}$ cluster to simulate the stiffness of the Si lattice, while all Si atoms and adsorbates and/or substitutional atoms were initially located near the center Si═Si dimer and then allowed to move as needed to minimize the total energy. Calculations were performed using the Gaussian 94/DFT program,[20] using the Becke3LYP hybrid density functional[21,22] (which includes a exchange-correlation effects) and the 6-31+G basis set. Some investigations were performed on smaller Si9 clusters and with larger basis sets (such as 6-31+G*) to help identify the relative importance of the size of the basis set and the size of the molecular cluster.

For PH_3 molecular adsorption two adsorption geometries were investigated. Figure 11 shows these geometries and some other adsorption fragments to be discussed below. Figure 11a depicts the Si═Si dimer of the clean surface. One possible PH_3 adsorption geometry is an "on-top" configuration in which the single P lone pair orbital interacts with the two Si atoms of a dimer as originally suggested by Yu et al.[14] (Figure 11b) and a "dangling bond" position in which the PH_3 molecule is adsorbed to one side of a dimer (Figure 11c). The energy of adsorption can then be calculated by subtracting the total energy of the $Si_{21}P_1H_{23}$ cluster from the combined energy of a $Si_{21}H_{20}$ surface modeling the dimerized Si(001) surface, and the total energy for a PH_3 molecule can be calculated using the same basis set. Calculations based on Si_9 and Si_{21} clusters both predicted that the stable PH_3 bonding site corresponds to the "dangling bond" position despite the unusual coordination number of 4 at this location. Using the 6-31+G basis set and the Becke3LYP hybrid density functional, the binding energy for PH_3 on the

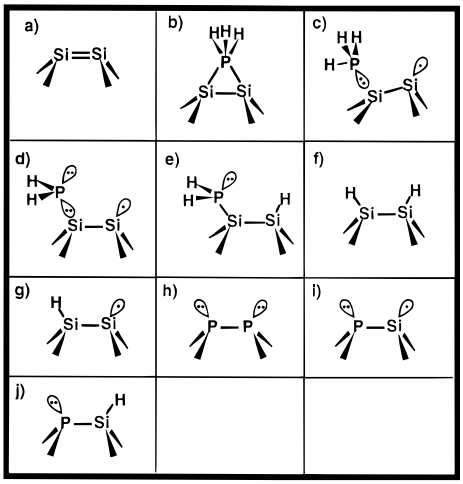

Figure 11. Schematic depiction of surface species and adsorbed fragments as described in the text. Unterminated bonds (black triangles) extend to the bulk Si lattice (not shown).

three-dimer Si_{21} cluster was 1.0 eV, compared with 0.6 eV for similar calculations using an Si_9 cluster.

The origin of the cluster size dependence seems to be that the large cluster permits more facile dimer tilting by having adjacent dimers tilt in the opposite direction, while the smaller Si_9 cluster constrains the tilting. The Si dimer atom bonded to the PH_3 cluster is pulled into the surface, while the unbonded Si atom is pushed outward into the vacuum, leading to a dimer tilt angle of 14° with respect to the macroscopic (100) plane for the Si_{21} cluster. Although dimer tilting is permitted in the Si_9 cluster, the termination of the cluster close to the molecular fragment constrains the amount of dimer tilting permitted and thereby affects the bonding energetics of PH_3. We note that analogous calculations using smaller basis sets and using only Hartree−Fock theory resulted in significantly larger binding energies for both small and large clusters. Thus, the discrepancy between the 1.0 eV bonding energy reported here for the Si_{21} cluster and 2.25 eV found by Cao et al.[17] is attributed to the fact that they utilized a smaller basis set and did not include correlation effects. Although Yu et al.[14] reported an activation barrier of approximately 0.6 eV for PH_3 desorption from Si(001) based on their temperature-programmed desorption (TPD) experiments, an examination of the published data suggests that the TPD peak may not be fit with a simple first-order Arrhenius-type desorption process with reasonable values for the enthalpy of desorption and preexponential factor. While more work needs to be done to resolve this discrepancy, it is clear the PH_3 is expected to bond to Si(001) in an intact molecular form at a dangling bond position and that the strength of this bond is on the order of 1 eV.

4. Discussion

IR Spectral Assignment: P−H Vibrations. In the section below we assign the vibrational features observed in Figures 1−10 with specific surface species, as depicted in Figure 12. This assignment is based on part on a comparison with gas-phase species. Experimental measurements of gas-phase silylphosphine compounds show that the frequency of the P−H stretching mode vibrations decreases when hydrogen atoms are replaced by silicon atoms, so that PH_3 has the highest frequencies (2321 and 2326 cm^{-1}), PH_2SiH_3 (silylphosphine) has a P−H frequency of 2312 cm^{-1}),[23] and $PH(SiH_3)_2$ (disilylphosphine) has a lower frequency of 2300 cm^{-1}.[24,25] Each successive substitution of H by Si shifts the P−H frequency by approximately 10−15 cm^{-1}. This shift appears to be quite characteristic in terms of the number of Si atoms bonded to the atom. For example, silylphosphine (SiH_3PH_2), bis(phosphino)-silane ($SiH_2(PH_2)_2$), and tris(phosphino)silane ($SiH(PH_2)_3$), all of which have one Si atom directly bonded to the P atom, show nearly the same P−H vibrational frequencies of approximately 2312, 2310, and 2308 cm^{-1}, respectively.[23,26,27] Thus, the approximate frequency of the P−H stretches appears to be a good fingerprint for the degree of substitution.

The vibrational spectrum for gas-phase phosphine shows one mode with A_1 character (C_{3v} point group) at 2321 cm^{-1} and a doubly degenerate mode with E character (point group C_{3v}) at 2326 cm^{-1}.[28] The vibrational spectrum for molecularly adsorbed phosphine has an unusual coordination number of four for the phosphorus atom when bonded onto a Si "dangling bond" site. The adsorption of molecular PH_3 onto a Si dimer with local C_{2v} symmetry will reduce the overall point group to C_s symmetry and remove the degeneracy of the E mode, so that three vibrational lines are predicted.

In all our spectra, we observe a set of three "group I" peaks at 2268, 2280, and 2290 cm^{-1}. These peaks have the same relative intensities irrespective of the method of preparation and/or sample temperature, indicating that they arise from the vibrations of a single chemical entity. Since a PH_2 group can only give rise to two stretching-type peaks and a PH group will only give rise to one, the observation of *three* P−H correlated vibrational peaks implies that these peaks arise from molecularly adsorbed PH_3. Thus, we concluded that the three "group I" peaks at 2268, 2280, and 2290 cm^{-1} arise from molecularly adsorbed PH_3.

Our conclusion that a significant amount of PH_3 is adsorbed molecularly on Si(001) is also supported by several other pieces of evidence. First, the flux-dependent dosing experiments (as in Figure 4) and annealing experiments (Figures 5−9) consistently show that the infrared peaks attributed to molecularly adsorbed PH_3 arise from the *initial* product of PH_3 adsorption on the Si(001) surface. Figures 7 and 8 show that the these peaks are eliminated by annealing temperatures above 475 K and are absent above 550 K. This is the same temperature range in which Colaianni et al.[18] observed desorption of molecular PH_3 from the surface in temperature-programmed desorption (TPD) experiments. In their studies, two desorption peaks were observed for PH_3 at 485 and 635 K. While isotopic mixing studies showed that the high-temperature peak at 635 K arose from recombinative desorption via the reaction $PH_{2(ads)} + H_{(ads)} \rightarrow PH_{3(gas)}$, they were unable to determine the origin of the lower temperature peak. Second, the peaks at 2280 and 2290 cm^{-1} are very close to the frequencies of 2285 and 2294 cm^{-1} observed for PH_3 adsorption on Si(111), as shown in Figure 10. Previous studies have shown strong evidence for the existence of molecularly adsorbed PH_3 on Si(111)-(7×7) up to 550 K.[8,9] Finally, we note that from experiments on phosphorus-enriched Si(001) (Figure 9c,d) these three peaks are by far the dominant P−H features; on clean Si samples (Figure 9a), these peaks are smaller, are accompanied by other P−H features, and are accompanied by a large increase in the Si−H vibrational intensity. We showed previously that on phosphorus-enriched surfaces the P atoms disperse on the surface to form P−Si heterodimers;[15] one consequence of this dispersal is that at intermediate phosphorus coverages the number of surface locations where two adjacent surface sites are available is quite small. Since PH_3 likely requires two adjacent surface sites to dissociate, then the phosphorus-enriched Si(001) surface is expected to stabilize the molecularly adsorbed PH_3, in agreement with what is observed in Figure 9c,d.

Assignment of the group II peaks at 2239, 2245, 2251, and 2261 cm^{-1} is slightly more complicated. At low to medium coverage, Figure 7 shows that these peaks increase in intensity at temperatures near 400 K, concurrent with the decrease in intensity of the 2280 cm^{-1} peak attributed to molecular PH_3-(ads). This indicates that these peaks are a decomposition product of PH_3. At saturation coverage (Figure 8) a smaller increase can be detected near 500 K, again concurrent with the decrease in intensity of the 2280 cm^{-1} peak of $PH_{3(ads)}$. At this coverage, the group II peaks disappear after annealing to 600−650 K; this is the same temperature range where Colaianni et al.[18] observed the disappearance of a PH_2 scissor mode at 1050 cm^{-1}. This temperature dependence suggests that these four peaks arise from PH_2 groups adsorbed on the surface. Closer analysis shows that the four lines can be divided into two sets of two lines. Figures 5 and 8 show that annealing the saturation coverage surface leads initally to the disappearance of the peaks at 2261 and 2239 cm^{-1}, leaving behind the two peaks at 2245 and 2251 cm^{-1}. Coverage-dependent studies show that the peaks at 2239 and 2261 cm^{-1} grow in at lower coverage, and those at 2245 and 2251 cm^{-1} grow in at higher coverage. This grouping into pairs of correlated lines suggests that these four peaks arise from the symmetric and asymmetric P−H stretching vibrations of two chemical forms of adsorbed PH_2, one giving rise to vibrations at 2245 and 2251 cm^{-1} and another to vibrations at 2239 and 2261 cm^{-1}.

Since at low coverage the surface consists primarily of bare Si sites, the most likely structure giving rise to the peaks at 2239 and 2261 cm^{-1} is the adsorption of a PH_2 group onto the "dangling bond" of a Si═Si dimer, as in Figure 11d. The peaks at 2245 and 2251 cm^{-1} grow in a higher coverage and/or after mild thermal annealing. Under these conditions the surface has a significant coverage of hydrogen due to dissociation of some of the PH_3, so that the most likely structure for the 2245 and 2251 cm^{-1} peaks is a PH_2 group adsorbed onto the dangling bond of a Si dimer which already has one hydrogen atom on it, as shown in Figure 11e. This structure would be expected to be more stable because it eliminates all surface dangling bonds, much like the additional stabilization of H in the "monohydride" structure.[29] Thus, at temperatures where hydrogen atoms have significant mobility, the most stable form of surface PH_2 is expected to be that in which it is paired with a hydrogen atom on the same dimer.

IR Spectral Assignment: Si−H Vibrations. The assignment of the PH frequencies is also complemented by an analysis of the Si−H frequencies. It is well-known that hydrogen atoms can order on Si(001) to form the Si(001)-(2×1)H "monohydride" structure shown in Figure 11f, in which each surface Si atom has one H atom bonded to it. Chabal[30−32] has shown that p-polarized infrared spectra of this structure show two sharp lines at 2087 and 2099 cm^{-1} that are attributed to the asymmetric and symmetric Si−H stretches. Using s-polarized light, only the asymmetric stretch at 2087 cm^{-1} is visible due to the surface infrared selection rules, which favor observation of species with transition dipoles parallel to the surface; the symmetric stretch has its transition dipole perpendicular to the surface and is therefore nearly invisible in s-polarized light.

We attribute the 2070 cm^{-1} peak to Si dimers in which a H atom is bonded to one Si atom, and the other atom of the dimer has a free "dangling bond", as shown in Figure 11g. A peak has previously been observed at this frequency by Chabal[33] for H/Si(001) and by Wu et al.[34] during thermal decomposition of disilane on Si(001). While both these studies attributed the 2070 cm^{-1} peak to H adsorbed at step edges or defect sites, we believe the previous assignment is incorrect. First, the intensity of the peak is very large, indicating that it accounts for a large fraction of the H on the surface. While Wu et al.[34] suggested that it could arise from SiH_2 groups, SiH_2 groups would normally be expected to give rise to two distinguishable peaks corresponding to the symmetric and antisymmetric modes; yet, only one line is observed. We have verified in our own laboratory that a large peak at exactly this frequency is produced during thermal decomposition of disilane, indicating that it is not directly associated with the presence of phosphorus. We believe that the most logical explanation for this vibrational mode is the structure shown in Figure 11g, with one H atom bonded on a surface dimer. We will refer to this structure as a "hemihydride", since the H/Si ratio is half that of the monohydride structure.

When annealing the PH_3-saturated surface to higher temperatures, the peak ascribed to the HSi−SiH monohydride specie is replaced by a single peak at approximately 2110 cm^{-1}. Because this peak is absent during desorption of hydrogen produced by thermal dissociation of disilane on Si(001),[34] we attribute it directly to the presence of surface phosphorus. A comparison of Figures 5 and 6 with Figure 9 shows that this peak is substantially increased in intensity when PH_3 interacts with Si(001) surfaces previously enriched with surface phosphorus. In a previous STM study[15] we showed that, during the phosphorus enrichment process used to prepare the starting substrates for Figure 9 and during thermal annealing of PH_3-exposed Si(001) surfaces, phosphorus atoms initially present on the terrace displace Si atoms for the surface Si═Si dimers. This creates P−Si "heterodimers" (Figure 11i) in the surface plane and ejects Si atoms onto the terraces, where they agglomerate together into Si═Si (and more P−Si) dimers. The P−Si heterodimer is formally a radical with one electron in a "dangling bond" on the Si atom; this specie is therefore moderately reactive, and surface H can bond at this danging bond site to form the P−SiH "hydrogenated heterodimer" (Figure 11j). This is supported by the fact that in Figure 9e (after annealing PH_3 adsorbed on the phosphorus-enriched surface) the 2110 cm^{-1} peak is the largest SiH peak visible in the spectrum. Thus, we propose that the Si−H mode at 2110 cm^{-1} arises from the hydrided heterodimer, a P−SiH unit. At very high surface phosphorus concentrations, Figure 9 shows that yet another peak can arise at 2124 cm^{-1}. We believe that this peak arises from a structure in which H is bonded to surface Si atom that is bonded to *two* phosphorus atoms. This peak is only observed at very high phosphorus concentrations.

Adsorption and Dissociation Mechanisms of PH_3 on Si-(001). Figure 13 summarizes the dissociation process for PH_3 on Si(001). Our flux-dependent studies show that the amount of molecular PH_3 on the surface is strongly dependent on the flux during exposure. This demonstrates that if sufficient surface sites are available, the molecularly adsorbed PH_3 can dissociate on a time scale of several minutes. If sufficient surface sites are *not* available, however, the molecularly adsorbed PH_3 is stable. Indeed, we have allowed PH_3-saturated surfaces to remain in our ultrahigh-vacuum chamber for more than 12 h, with negligible change in the infrared spectrum. Thermal annealing studies as shown in Figures 4 and 5 also show that at high coverage the PH_3 is stable to higher temperatures, presumably because of the unavailability of nearly sites. The inability of phosphine to dissociate at high coverage is somewhat surprising in light of the fact that at least three independent studies of phosphine interaction with Si(001) have shown that the saturation coverage is approximately 0.25 monolayer.[12,14−16,18] Since this is significantly lower than 1 monolayer, the stability of molecularly adsorbed PH_3 at satura-

System	Structure	Mode	Frequency (cm^{-1})	Reference
PH_3/Si(001)	H_3P Si–Si	P-H3 P-H3 P-H3	2268 2280 2290	This work
PH_2/Si(001)	H_2P Si–Si H	P-H2 s P-H2 as	2245 2251	This work
PH_2/Si(001)	H_2P Si–Si ⊙	PH2 s PH2 as	2239 2261	This work
PH_3 gas	PH_3	P-H3 (A1) P-H3 (E)	2321 2326	Ref. 32
SiH_3PH_2 gas (Silylphospine)	H_3Si-PH_2	PH2	~2312	Ref. 30
$SiH_2(PH_2)_2$ gas (Bis(phosphino-)silane)	SiH_2 H_2P PH_2	PH2	2310	Ref. 31
$SiH(PH_2)$ gas (Tris(phosphino-)silane)	SiH PH_2 PH_2 PH_2	PH2	2308	Ref. 31
PH_3/Si(001) H/Si(001)	H Si–Si H	H-Si-Si-H as H-Si-Si-H s	2087 2099	This work (PH3) Chabal (H)
PH_3/Si(001)	⊙ Si–Si H	db-Si-Si-H	2060-2070	This work
PH_3/Si(001)	H_2P Si–Si H	Si-H	2093	This work
PH_3/Si(001)	H P–Si	Si-H	2109-2115	This work

Figure 12. Assignment of infrared spectral features observed in this study and comparison with some experimental values for related surface and gas-phase compounds.

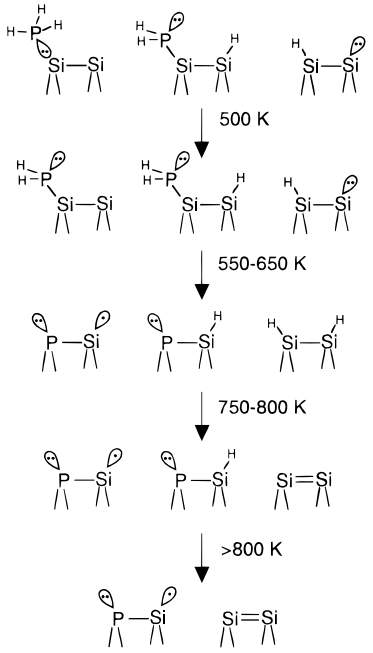

Figure 13. Summary of PH_3 decomposition mechanism on Si(001).

tion exposure cannot be entirely accounted for by simple site counting but must also involve significant steric interactions that prevent the PH_3 from dissociating when packed into the ordered c(4×2) configuration observed in our previous STM studies.

Our quantum chemistry calculations indicate that the bonding strength of PH_3 on Si(001) is increased by dimer tilting. As noted above, the Si atom bonded to the PH_3 recesses into the surface (toward the bulk), while its phosphorus partner protrudes from the surface. It has long been known[35] that dimer tilting involves electron transfer from the protruding atom to the recessing atom, and STM studies of tilted dimers show that the density of occupied states is higher on the protruding atom and lower on the recessing atom.[36] This in turn implies that the up atom is an electron-donating site, and the down atom is an electron-withdrawing or nucleophilic site. Thus, the lone pair electrons of PH_3 more readily bond to the nucleophilic "down" atom of a tilted dimer, as depicted in Figure 11c. The correlated tilting of dimers along a given row may also explain why STM images[16] show that PH_3 molecules on Si(001) tend to adsorb into rowlike structures: since the Si(001) dimer tilting is also highly correlated in this direction, the first PH_3 adsorption event will cause dimer tilting at other locations along the same dimer row; this in turn creates more electrophilic (and nucleophilic) sites at tilted dimers, increasing the probability of subsequent PH_3 molecules adsorbing in this same row.

The extent of dissociation of PH_3 can be crudely estimated from an analysis of the relative areas of PH_3 and PH_2 infrared absorption peaks. While polarization-dependent spectra show some changes in the relative intensities of the P−H lines (and hence the influence of surface orientation effects and dipole selection rules), we expect that the predominant factor influencing the relative intensities of the group I vs group II lines is the number of fragments of either type on the surface. A comparison of the relative areas of the PH_2 (group II) and PH_3 (group I) features in Figure 6 suggests that at low flux approximately 40% of the incident PH_3 might dissociate, while at high flux the fraction dissociation can be <10%. We also note that although the Si−H stretch appears to dominate the infrared spectra, our results suggest that this is an artifact of the unusually high infrared transition dipole for Si−H. If the only surface species are $H_{(ads)}$, $PH_{2(ads)}$, and $PH_{3(ads)}$, then the absolute number of Si−H species will be equal to the number of PH_2 groups. A comparison of the relative areas of the Si−H peaks and the PH_2 peaks then yields the relative infrared transition strengths for Si−H and PH_2. Integration of the areas assigned to PH_2 and Si−H features in Figure 3 suggests that the surface IR transition dipole for Si−H is approximately 5−6 times that of the combined (symmetric + antisymmetric) P−H lines. Thus, the observation of a Si−H in a spectroscopic probe such as IR can easily lead to the mistaken conclusion that dissociation is extensive, while our results show that most of the PH_3 can be adsorbed in the molecular state under suitable conditions.

As noted above, the extent of dissociation is likely to be affected not only by the flux rate but also by the presence of defects on the surface. In a previous scanning tunneling microscopy study, we showed that PH_3 strongly reacts at defects, ejecting Si adatoms onto the surface and enlarging vacancy defects.[16] In contrast, on flat, free regions we observed the formation of arrays of protrusions (which we assigned to molecularly adsorbed PH_3) ordered into a local c(4×2) arrangement. On the basis of this observation, we therefore expect that the extent of dissociation will be strongly enhanced by the presence of defects on the surface.

Dissociation of PH_3 produces $PH_{2(ads)}$ and $H_{(ads)}$ on the surface. After dissociation to $PH_{2(ads)} + H_{(ads)}$ has taken place, further dissociation again requires the availability of more free surface sites. Once again, the PH_2 species are stabilized at high coverage, decomposing about 500 K at low coverage (Figure 4) but decomposing only above 625−650 K at high coverage (Figure 5). In this temperature range, we find that the decrease in the intensity of IR peaks assigned to PH_2 groups is not accompanied by the formation of any new IR peaks. This in turn suggests that $PH_{2(ads)}$ decomposes immediately to $P_{(ads)} + 2H_{(ads)}$ (with some H_2 likely going into the gas phase) and that there is no stable $PH_{(ads)}$ intermediate. Although our calculations indicate the $PH_{(ads)}$ is a possible stable intermediate, neither our

studies nor previous EELS studies[18] have provided any evidence for its existence.

The temperature range at which $PH_{2(ads)}$ dissociates is close to the temperature at which significant H atom diffusion occurs. As the temperature increases above 650 K, the H atoms produced by the initial dissociation of PH_3 or by subsequent dissociation of $PH_{2(ads)}$ are able to pair on the Si dimers, forming the Si(001)-(2×1)H monohydride structure. This leads to a decrease in the hemihydride peak at 2070 cm^{-1} and a concurrent increase in the monohydride peaks at 2087 and 2090 cm^{-1}. The large changes in the Si−H spectra associated with this transition from hemihydride to monohydride structure make it difficult to quantitatively analyze the amount of surface hydrogen present on the surface in this temperature range.

By a temperature of approximately 700 K, all PH_x species have dissociated into gas-phase H_2 and surface P. As noted above, in this temperature range the only Si−H vibrational feature is from the P−SiH hydrided heterodimer (Figure 11g) structure. It is significant to note that the temperature at which hydrogen desorbs from this structure is significantly higher than the desorption temperature of H from clean Si(001). This may partially explain the decrease reactivity observed in CVD processing in which P is incorporated as a dopant.[1−4]

5. Summary

We have studied the adsorption and decomposition of PH_3 on Si(001). Our results show the presence of several distinct phosphorus-containing species. Detailed analysis of the spectra, in conjunction with ab initio total energy calculations, provides insight into the energetics of these species. Our results show the presence of several chemically distinct forms of phosphorus on the surface. The initial adsorption of phosphine occurs through two competing channels, leaving the surface with both molecularly adsorbed PH_3 and dissociation fragments, which are attributed primarily to $PH_{2(ads)} + H_{(ads)}$. The branching into these channels is dependent on the exposure flux and total coverage and molecular species more stable at high coverage and high flux exposure. The ability of infrared spectroscopy to detect even small changes in chemical environment has permitted a detailed analysis of the chemical species present during decomposition of PH_3 on Si(001). The integration of this infrared data with previous scanning tunneling microscopy data on the spatial distribution of H and P on Si(001) surfaces provides a coherent model for the decomposition mechanism.

Acknowledgment. The authors thank Professor Frank Weinhold for his assistance in the use of the Gaussian 92 program. This work is supported in part by the U.S. Office of Naval Research and by the National Science Foundation. Some computer time was provided by the NSF National Center for Supercomputer Applications under Grant CHE950029N.

References and Notes

(1) Eversteyn, F.; Put, B. H. *J. Electrochem. Soc.* **1973**, *120*, 106−110.
(2) Chang, C. A. *J. Electrochem. Soc.* **1976**, *123*, 1245−1247.
(3) Kurokawa, H. *J. Electrochem. Soc.* **1982**, *129*, 2620−2624.
(4) Meyerson, B. S.; Olbricht, W. *J. Electrochem. Soc.* **1984**, *131*, 2361−2365.
(5) van Bommel, A. J.; Meyer, F. *Surf. Sci.* **1967**, *8*, 381.
(6) van Bommel, A. J.; Crombeen, J. E. *Surf. Sci.* **1973**, *36*, 773−777.
(7) Bozso, F.; Avouris, P. *Phys. Rev. B* **1991**, *43*, 1847−1850.
(8) Taylor, P. A.; Wallace, R. M.; Choyke, W. J.; Yates, J. T., Jr. *Surf. Sci.* **1990**, *238*, 1−12.
(9) Wallace, R. M.; Taylor, P. A.; Choyke, W. J.; Yates, J. T., Jr. *J. Appl. Phys.* **1990**, *68*, 3669−3678.
(10) Chen, P. J.; Colaianni, M. L.; Wallace, R. M.; Yates, J. T., Jr. *Surf. Sci.* **1991**, *244*, 177−184.
(11) Meyerson, B. S.; Yu, M. L. *J. Electrochem. Soc.* **1984**, *131*, 2366−2366.
(12) Yu, M. L.; Meyerson, B. S. *J. Vac. Sci. Technol. A* **1984**, *2*, 446−449.
(13) Yu, M. L.; Vitkavage, D. J.; Meyerson, B. S. *J. Vac. Sci. Technol. A* **1985**, *3*, 861−862.
(14) Yu, M. L.; Vitkavage, D. J.; Meyerson, B. S. *J. Appl. Phys.* **1986**, *59*, 4032−4037.
(15) Wang, Y.; Chen, X.; Hamers, R. J. *Phys. Rev. B* **1994**, *50*, 4534−4547.
(16) Wang, Y.; Bronikowski, M. J.; Hamers, R. J. *J. Phys. Chem.* **1994**, *98*, 5966−5973.
(17) Cao, P. L.; Lee, L. Q.; Dai, J. J.; Zhou, R. H. *J. Phys.: Condens. Matter* **1994**, *6*, 6103−6109.
(18) Colaianni, M. L.; Chen, P. J.; Yates, J. T., Jr. *J. Vac. Sci. Technol. A* **1994**, *12*, 2995−2998.
(19) Hamers, R. J.; Wang, Y.; Shan, J. Manuscript in preparation.
(20) Frisch, M. J.; G. W. T., Schlegel, H. B.; Gill, P. M. W.; Johnson, B. G.; Wong, M. W.; Foresman, J. B.; Robb, M. A.; Head-Gordon, M.; Replogle, E. S.; Gomperts, R.; Andres, J. P.; Raghavachari, K.; Binkley, J. S.; Gonzalez, C.; Martin, R. L.; Fox, D. J.; Defre, D. J. *Gaussian 94/DFT*; Gaussian Inc.: Pittsburgh, PA, 1993.
(21) Becke, A. D. *J. Chem. Phys.* **1993**, *98*, 5648.
(22) Lee, C.; Yang, W.; Parr, R. G. *Phys. Rev. B* **1988**, *37*, 785.
(23) Drake, J. E.; Riddle, C. *Spectrochim. Acta* **1970**, *26A*, 1697−1706.
(24) Gokhale, S. D.; Jolly, W. L. *Inorg. Chem.* **1964**, *4*, 596−597.
(25) Gokhale, S.; Jolly, W. L. *Inorg. Chem.* **1964**, *3*, 1141−1143.
(26) Linton, H. R.; Nixon, E. R. *Spectrochim. Acta* **1967**, *23A*, 2713.
(27) Norman, A. *J. Am. Chem. Soc.* **1968**, *90*, 6556−6557.
(28) Tarrago, G.; Lacome, N.; Levy, A.; Guelachvili, G.; Bezard, B.; Drossart, P. *J. Mol. Spectrosc.* **1992**, *154*, 31−42.
(29) Boland, J. J. *Phys. Rev. Lett.* **1991**, *67*, 1539.
(30) Chabal, Y. J. *Surf. Sci.* **1986**, *168*, 594−608.
(31) Chabal, Y. *Surf. Sci. Rep.* **1988**, *8*, 211−357.
(32) Chabal, Y. J.; Higashi, G. S.; Raghavachari, K.; Burrows, V. A. *J. Vac. Sci. Technol. A* **1989**, *7*, 2104−2109.
(33) Chabal, Y. J.; Raghavachari, K. *Phys. Rev. Lett.* **1984**, *53*, 282.
(34) Wu, Y. M.; Baker, J.; Hamilton, P.; Nix, R. M. *Surf. Sci.* **1993**, *295*, 133−142.
(35) Chadi, D. J. *Phys. Rev. Lett.* **1979**, *43*, 43.
(36) Hamers, R. J.; Tromp, R. M.; Demuth, J. E. *Surf. Sci.* **1987**, *181*, 246−355.

JP952452H